Influence of Nitrogen Content on Persistent Photoconductivity in Zinc Oxynitride Thin Film Transistors

Jun Tae Jang, Hyoung-Do Kim, Dong Myong Kim, *Member, IEEE*, Sung-Jin Choi, Hyun-Suk Kim, and Dae Hwan Kim, *Senior Member, IEEE*

***Abstract*— In this work, the influence of anion composition on the photoresponse characteristics of zinc oxynitride thin film transistors is investigated and compared directly to conventional In-Ga-Zn-O TFTs. Increasing the ratio of N to (N+O) led to higher field effect mobility and improved subthreshold swing. The subgap density of states extracted by monochromatic photonic capacitance-voltage measurement indicated that the nitrogen-related defect states, such as nitrogen vacancies, increased with increasing nitrogen gas flow rate. Furthermore, the photoconductivity mechanism of ZnON TFTs is discussed in detail.**

***Index Terms*— Zinc oxynitride (ZnON), anion composition, persistent photoconductivity (PPC), subgap density of states (DOS).**

I. Introduction

INCREASING demands for low-cost switching or driving transistors by the flat panel display industry have led to the development of amorphous metal oxide based semiconductors (AOSs), such as In-Ga-Zn-O (IGZO) [1]. Compared to amorphous silicon, thin film transistors (TFT) based on AOSs exhibit relatively high field effect mobility (> 10 cm^2/Vs), and are suitable for large size and high resolution active matrix light emitting diode panel [1]. However, most AOSs inevitably contain oxygen-related defects, such as oxygen vacancies (V_Os) that may induce persistent photoconductivity (PPC) problems under illumination [2], [3].

Recently, a relatively new type of semiconductor, zinc oxynitride (ZnON), succeeded in obtaining high mobility (> 50 cm^2/Vs) [2], [4]–[7]. In addition, ZnON is fabricated through a simple and cost-effective process using reactive sputtering with a Zn metal target. The optimization of the associated TFT properties to obtain sufficiently low leakage current levels while maintaining high field effect mobility usually consists of controlling either the anion composition ratio [8], [9] or the doping process [10, 11] in the ZnON layer. It has also been reported that ZnON TFTs exhibit excellent stability with suppressed PPC effects under illumination [3]. It is suggested that the incorporation of nitrogen into ZnO shifts the valence band maximum (VBM) level upwards, effectively passivating the V_Os [4], [7]. Nevertheless, the influence of anion composition on the PPC effects and the change in subgap density of states (DOS) in ZnON have scarcely been investigated.

In this work, the PPC phenomenon of ZnON TFTs with various anion compositions was investigated with subgap DOS analysis. The subgap DOS of each device was extracted by the monochromatic photonic capacitance-voltage (MPCV) technique. The anion composition of ZnON was modulated by the flow rate of reactant gas during the sputter deposition. Extracted subgap DOS distribution indicated that the nitrogen-related defect states (V_Ns) strongly affect the PPC of ZnON Furthermore, the PPC mechanism of ZnON TFTs is compared in detail to that of conventional amorphous IGZO TFTs.

II. Experiments

Firstly, bottom gate IGZO and ZnON TFTs were fabricated using a glass substrate. A 200-nm-thick Mo was utilized for the bottom gate, and deposited by direct-current (DC) sputtering at room temperature. The gate dielectrics of 350-nm-thick SiN_x and 50-nm-thick SiO_x were then deposited using plasma-enhanced chemical vapor deposition (PECVD) at 350 °C. The ZnON active layer with a thickness of 50 nm was deposited through reactive radio-frequency (RF) magnetron sputtering using a Zn metal target and N_2 and O_2 gas reactants. To control the anion composition, the gas flow ratio of Ar:O_2:N_2 (sccm) was modulated as 10:2:100, 10:3:100, and 10:4:100, corresponding to N/(N + O) ratios of 85 %, 80 %, and 60 %, respectively, based on Rutherford backscattering spectrometry analysis. Deposition of the IGZO (50 nm-thick) utilized DC sputtering with an $In_2Ga_2ZnO_7$ target. The gas mixture ratio of Ar:O_2 (sccm) was fixed at 35:20. After active layer deposition, a 100-nm-thick SiO_x etch-stop layer was deposited at 200 °C

Manuscript received January 17, 2020; accepted February 13, 2020. Date of publication February 18, 2020; date of current version March 24, 2020. This work was supported by the National Research Foundation of Korea (NRF) through the Ministry of Education, Science and Technology (MEST), Korean Government, under Grant 2016R1A5A1012966, Grant 2017R1A2B4006982, Grant 18ZB1800, Grant 2016M3A7B4909668, and Grant NRF-2019R1I1A2A01064153. The review of this letter was arranged by Editor D. Shahrjerdi. *(Corresponding authors: Hyun-Suk Kim; Dae Hwan Kim.)*

Jun Tae Jang, Dong Myong Kim, Sung-Jin Choi, and Dae Hwan Kim are with the School of Electrical Engineering, Kookmin University, Seoul 136-702, South Korea (e-mail: drlife@kookmin.ac.kr).

Hyoung-Do Kim and Hyun-Suk Kim are with the Department of Materials Science and Engineering, Chungnam National University, Daejeon 305-764, South Korea (e-mail: khs3297@cnu.ac.kr).

Color versions of one or more of the figures in this letter are available online at http:ieeexplore.ieee.org.

Digital Object Identifier 10.1109/LED.2020.2974757

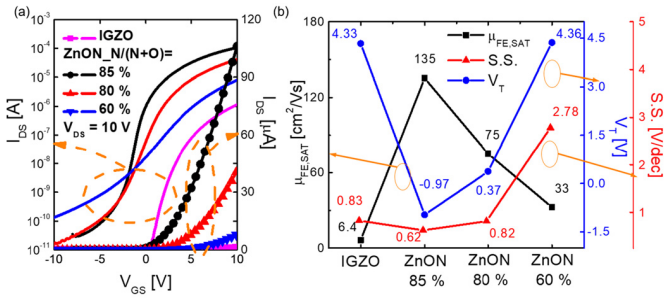

Fig. 1. (a) Transfer curves and (b) extracted threshold voltage, subthreshold swing, and field effect mobility of IGZO and ZnON TFTs.

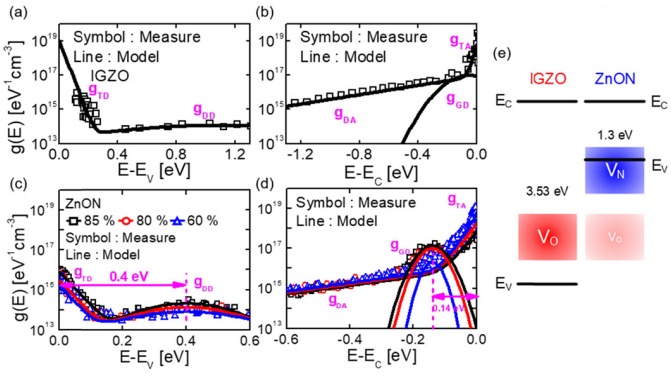

Fig. 2. Experimentally extracted subgap DOS profiles of (a), (b) IGZO and (c), (d) ZnON near (a), (c) VBM and (b), (d) near CBM. (e) Schematic band diagram of IGZO and ZnON (60 %).

through PECVD. Finally, DC sputtering was used to deposit a 100 nm-thick Mo (IGZO) and AlNd (ZnON) source/drain layer. The channel layer width/length was 50μm /50μm. The post annealing process was performed in air for one hour at 250 °C.

All electrical properties were measured using an Agilent 4156C precision semiconductor parameter analyzer. The photoresponse property of the drain current (I_{DS}) was observed using a laser source with a wavelength of 532 nm. Capacitance-voltage (C-V) data was measured using an HP 4284A precision LCR meter. The subgap DOS of each IGZO and ZnON TFT was extracted using the MPCV technique [12]. The conditions for the C-V characteristics were as follows: λ_{ph} = 440 nm (IGZO), 1064 nm (ZnON), P_{op} = 4 mW (IGZO), 2 mW (ZnON), and AC signal frequency = 50 kHz (IGZO), 10 kHz (ZnON).

III. Results and Discussion

Fig. 1(a) shows the electrical characteristics of IGZO and ZnON TFTs. Here, transfer curves of the ZnON TFTs are illustrated with different N/(N+O) ratios: ZnON (85 %), ZnON (80 %), and ZnON (60 %). The extracted transfer parameters of threshold voltage (V_{th}), subthreshold swing (S.S.), and field effect mobility (μ_{FE}) for each TFT are depicted in Fig. 1(b). In the ZnON TFTs, as the N/(N+O) ratio increases, the μ_{FE} is increased, while the S.S. and V_{th} become lower.

The extracted subgap DOS of IGZO and ZnON TFTs with different N/(N + O) ratios is illustrated in Fig. 2(a)–2(d). The

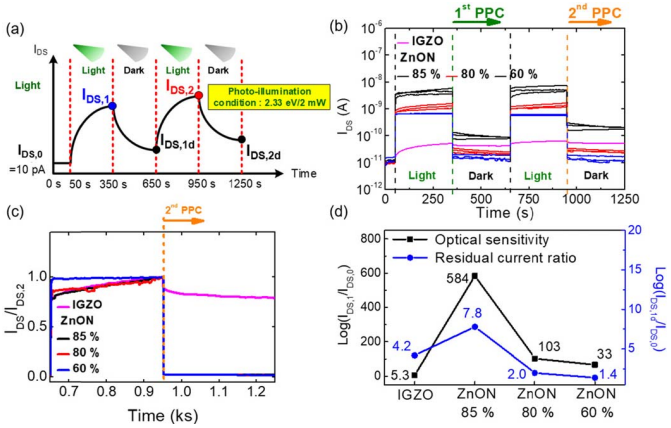

Fig. 3. (a) Experimental method for PPC test. (b) Photocurrent as a function of time, (c) normalized current levels of 2nd PPC test and (d) calculated optical sensitivity and residual current ratio of IGZO and ZnON TFTs.

DOS profile is found to be well fitted with the exponential shape and Gaussian peak. In the IGZO case, the g_D(E), which corresponds to V_o states, is dispersed in the band gap energy. The g_D(E) near the conduction band minimum (CBM) indicates ionized V_o states [13–15]. Similarly, ZnON also exhibits g_A(E) and g_D(E) regardless of the N/(N+O) ratio, which corresponds to V_Ns and ionized V_Ns, respectively [16]. Moreover, the g_D(E) of ZnON increased with respect to the N/(N+O) ratio, suggesting that the V_Ns is increased. Fig. 2(e) shows the band structure of IGZO and ZnON (60 %), indicating the location of possible defects in IGZO and ZnON.

Fig. 3(a) shows the experimental method for evaluating the PPC test, in which the duration of each light (illumination) and dark (recovery) state was fixed at 300 s. The energy of irradiated light onto IGZO and ZnON TFTs for testing PPC was same (E_{ph} = 2.33 eV). Fig. 3(b) shows the photoresponse of IGZO and ZnON TFTs, where three devices of ZnON TFTs with each N/(N+O) ratio were used for accurate PPC test results. Firstly, IGZO TFTs, as expected, displayed a gradually increasing photocurrent and a high PPC that originated from ionization of V_o states. The PPC of ZnON TFTs increased when the N/(N + O) ratio increases, i.e., of ZnON (85 %) TFTs demonstrated higher PPC, while in ZnON (60 %) TFTs exhibited negligible PPC. Fig 3(c) shows the normalized current level of the IGZO and ZnON devices after the second PPC test as a function of time. Fig. 3(d) shows the optical sensitivity ($\log(I_{DS,1}/I_{DS,0})$) and residual current ratio ($\log(I_{DS,1d}/I_{DS,0})$) of the IGZO and ZnON TFTs, where $I_{DS,0}$, $I_{DS,1}$, and $I_{DS,1d}$ indicate the initial off-state current before PPC test (10 pA), the photocurrent after 1st illumination (300 s), and the residual current after recover time (600 s), respectively. All ZnON TFTs exhibited higher optical sensitivity compared to IGZO TFTs. Additionally, while the residual current ratio of ZnON (85 %) was slightly higher than those of IGZO TFTs, IGZO TFTs showed the slowest recovery when the light source was removed, as seen in Fig. 3(b) and (c).

To investigate the origin of PPC in ZnON, the subgap DOS was extracted before and after the PPC test, where

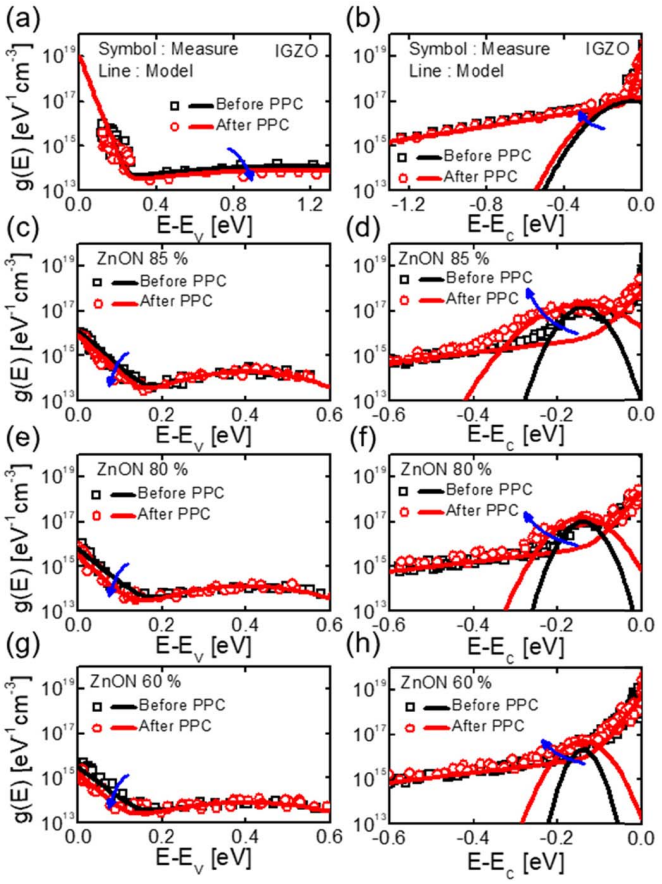

Fig. 4. Experimentally extracted subgap DOS of (a), (b) IGZO, (c), (d) ZnON 85%, (e), (f) ZnON 80%, and (g), (h) ZnON 60% before/after PPC test, (a), (c), (e), (g) near VBM and (b), (d), (f), (h) near CBM.

each N/(N+O) ratio were used for accurate extraction results. Figs. 4(a)–4(h) show the g(E) distribution of IGZO and ZnON TFTs before and after the PPC test. After the PPC test, the V_o ionization results for the IGZO reveal that the $g_D(E)$ near to VBM slightly decreased and $g_D(E)$ near to CBM slightly increased. Similarly, the $g_D(E)$ near the VBM level decreased for all ZnON TFTs. Conversely, large values of $g_D(E)$ near the CBM were observed in ZnON TFTs after the PPC test. Therefore, the PPC of ZnON TFTs may originate from the ionized V_Ns.

The schematic illustration of the carrier generation mechanism and the photoresponse behavior during PPC test of IGZO and ZnON TFTs is shown in Fig. 5. As demonstrated by Fig. 5(a), the PPC of IGZO mainly originates from the ionization of V_Os when a light source with 2.33 eV is used. It has been reported that the V_Os trap the holes in ZnO-based semiconductors, thus prevent electron-hole recombination after illumination. The defect ionization is a dominant component in this case, which causes PPC in IGZO. Accordingly, such defect-dependent carrier generation appears as the slow recovery regime during the PPC test. However, as shown in Fig. 5(b), the light energy of 2.33 eV is quite large compared to band gap energy of ZnON. Therefore, two types of carrier generation models are anticipated as follows: (i) band-to-band generation, and (ii) ionization of V_Ns. Generally, the

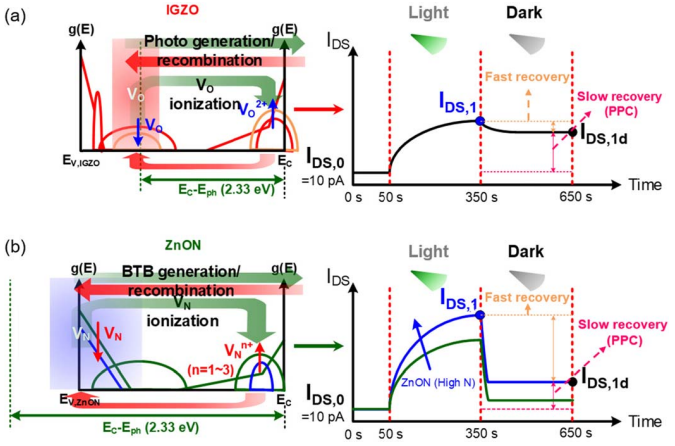

Fig. 5. Schematic diagram of carrier generation mechanism and the photoresponse behavior during PPC test of (a) IGZO and (b) ZnON.

band-to-band generation in AOS does not significantly affect the PPC phenomenon, as these generated carriers recombined immediately when the light source was turned off. Accordingly, band-to-band carrier generation represents the fast recovery regime in PPC test. Moreover, it suggests that an ionized V_N is the main component in the slow recovery region for ZnON PPC. Similar to V_Os, V_Ns may prevent the recombination of electrons and holes. This results in an increased slow recovery region as the nitrogen content ratio in the ZnON layer is increasing.

IV. Conclusion

In this work, the effects of anion composition ratio on the subgap DOS and PPC effects of ZnON TFTs were investigated. The extracted subgap DOS revealed that the nitrogen-related defect states, such as V_Ns, increased with increasing nitrogen flow rate during the sputtering process. Moreover, these increased V_Ns caused more severe PPC effects, which can be considered similar to the V_o dependent PPC phenomenon in IGZO. Therefore, controlling V_Ns using subgap DOS analysis represents a very important step for obtaining high performance and PPC-free ZnON TFTs.

References

[1] T. Matsuo, S. Mori, A. Ban, and A. Imaya, "Advantages of IGZO oxide semiconductor," in *SID Symp. Dig. Tech. Papers*, vol. 45, no. 1, Jun. 2014, pp. 83–86, doi: 10.1002/j.2168-0159.2014.tb00023.x.

[2] J. T. Jang, J. Park, B. D. Ahn, D. M. Kim, S.-J. Choi, H.-S. Kim, and D. H. Kim, "Study on the photoresponse of amorphous In–Ga–Zn–O and zinc Oxynitride semiconductor devices by the extraction of sub-gap-state distribution and device simulation," *ACS Appl. Mater. Inter.*, vol. 7, no. 28, pp. 15570–15577, Jul. 2015, doi: 10.1021/acsami.5b04152.

[3] S. Lee, A. Nathan, S. Jeon, and J. Robertson, "Oxygen defect-induced metastability in oxide semiconductors probed by gate pulse spectroscopy," *Sci. Rep.*, vol. 5, no. 1, p. 14902, Oct. 2015, doi: 10.1038/srep14902.

[4] H.-S. Kim, S. H. Jeon, J. S. Park, T. S. Kim, K. S. Son, J.-B. Seon, S.-J. Seo, S.-J. Kim, E. Lee, J. G. Chung, H. Lee, S. Han, M. Ryu, S. Y. Lee, and K. Kim, "Anion control as a strategy to achieve high-mobility and high-stability oxide thin-film transistors," *Sci. Rep.*, vol. 3, no. 1, p. 1459, Mar. 2013, doi: 10.1038/srep01459.

[5] E. Lee, A. Benayad, T. Shin, H. Lee, D.-S. Ko, T. S. Kim, K. S. Son, M. Ryu, S. Jeon, and G.-S. Park, "Nanocrystalline ZnON; high mobility and low band gap semiconductor material for high performance switch transistor and image sensor application," *Sci. Rep.*, vol. 4, no. 1, p. 4948, May 2014, doi: 10.1038/srep04948.

[6] J. Park, Y. S. Kim, K.-C. Ok, Y. C. Park, H. Y. Kim, J.-S. Park, and H.-S. Kim, "A study on the electron transport properties of ZnON semiconductors with respect to the relative anion content," *Sci. Rep.*, vol. 6, no. 1, p. 24787, Apr. 2016, doi: 10.1038/srep24787.

[7] J. Tae Jang, H. Kang, H. Ri Yu, E. Su Kim, K. Seok Son, S.-H. Cho, D. Myong Kim, S.-J. Choi, and D. Hwan Kim, "The influence of anion composition on subgap density of states and electrical characteristics in ZnON thin-film transistors," *IEEE Electron Device Lett.*, vol. 40, no. 1, pp. 40–43, Jan. 2019, doi: 10.1109/LED.2018.2883732.

[8] H. Jeong, H.-S. Jeong, D.-H. Kim, C.-Y. Jeong, and H.-I. Kwon, "Effects of post-deposition thermal annealing temperature on electrical properties of ZnON thin-film transistors," *IEEE Electron Device Lett.*, to be published, doi: 10.1109/LED.2016.2559523.

[9] J. Park, Y. S. Kim, J. H. Kim, K. Park, Y. C. Park, and H.-S. Kim, "The effects of active layer thickness and annealing conditions on the electrical performance of ZnON thin-film transistors," *J. Alloys Compounds*, vol. 688, pp. 666–671, Dec. 2016, doi: 10.1016/j.jallcom.2016.07.245.

[10] H.-D. Kim, J. H. Kim, K. Park, J. H. Kim, J. Park, Y. J. Kim, and H.-S. Kim, "Effects of fluorine doping on the electrical performance of ZnON thin-film transistors," *ACS Appl. Mater. Interfaces*, vol. 9, no. 29, pp. 24688–24695, Jul. 2017, doi: 10.1021/acsami.7b03385.

[11] H. Tsuji, T. Takei, M. Nakata, M. Miyakawa, and Y. Fujisaki, "Effects of tantalum doping on electrical characteristics of high-mobility zinc oxynitride thin-film transistors," *IEEE Electron Device Lett.*, vol. 40, no. 9, pp. 1435–1438, Sep. 2019, doi: 10.1109/LED.2019.2930062.

[12] H. Bae, H. Choi, S. Jun, C. Jo, Y. H. Kim, J. S. Hwang, J. Ahn, S. Oh, J.-U. Bae, S.-J. Choi, D. Hwan Kim, and D. Myong Kim, "Single-scan monochromatic photonic capacitance-voltage technique for extraction of subgap DOS over the bandgap in amorphous semiconductor TFTs," *IEEE Electron Device Lett.*, vol. 34, no. 12, pp. 1524–1526, Dec. 2013, doi: 10.1109/LED.2013.2287511.

[13] B. Ryu, H.-K. Noh, E.-A. Choi, and K. J. Chang, "O-vacancy as the origin of negative bias illumination stress instability in amorphous In–Ga–Zn–O thin film transistors," *Appl. Phys. Lett.*, vol. 97, Jun. 2010, Art. no. 022108, doi: 10.1063/1.3464964.

[14] J. G. Um, M. Mativenga, and J. Jang, "Mechanism of positive bias stress-assisted recovery in amorphous-indium-gallium-zinc-oxide thin-film transistors from negative bias under illumination stress," *Appl. Phys. Lett.*, vol. 103, no. 3, Jul. 2013, Art. no. 033501, doi: 10.1063/1.4813747.

[15] H. Oh, S.-M. Yoon, M. K. Ryu, C.-S. Hwang, S. Yang, and S.-H. Park, "Photon-accelerated negative bias instability involving subgap states creation in amorphous In–Ga–Zn–O thin film transistor," *Appl. Phys. Lett.*, vol. 97, Oct. 2010, Art. no. 183502, doi: 10.1063/1.3510471.

[16] T. S. Kim, H.-S. Kim, J. S. Park, K. S. Son, E. S. Kim, J.-B. Seon, S. Lee, S.-J. Seo, S.-J. Kim, S. Jun, K. M. Lee, D. J. Shin, J. Lee, C. Jo, S.-J. Choi, D. M. Kim, D. H. Kim, M. Ryu, S.-H. Cho, and Y. Park, "High performance gallium-zinc oxynitride thin film transistors for next-generation display applications," in *Proc. IEEE Int. Electron Devices Meeting*, Dec. 2013, p. 27, doi: 10.1109/IEDM.2013.6724701.